Comparative Evaluation and Refinement of Algorithm for Water Depth Estimation using Medium Resolution Remote Sensing Data

Vinayaraj, P.,[1] Raghavan, V.,[1] Masumoto, S.[2] and Glejin, J.[3]
[1]Graduate School for Creative Cities, Osaka City University, Japan
[2]Graduate School of Science, Osaka City University, Japan
[3]National Institute of Oceanography, Goa, India,
E-mail: vinay223333@gmail.com

Abstract

Information concerning water depth of near shore water region is one of the most basic requirements for coastal zone management. Depth is especially important for near coastal lines, in harbors, and near shoals and banks, where changes can occur rapidly as sedimentation, erosion and scouring of channels alters underwater topography. Although, the algorithms used to estimate depth from passive Remote Sensing (RS) satellite data were practicing last two decades, it is necessary to test the algorithms with recently available better quality RS data archives. In addition to that this paper proposes two methods to estimate water depth from single spectral band and from multispectral band. The single band algorithm called Radiance Based Estimation (RBE) is a modification of Stoffle and Halmo, (1991). Here onwards the single band method proposed by Stoffle and Halmo, (1991) is referred to as SLR (Single-band Linear Regression). A constant attenuation coefficient of a particular band is estimated using SLR method with limited in-situ depth; further the RBE is used to estimate depth from same band of multi-temporal images even when there is no in-situ depth available. RBE only depends upon the radiance value of the log-transformed band. The single spectral band from each satellite imagery is captured at different time is used to estimate multi-temporal depth from multi-source optical RS data such as Landsat 7, Landsat 8 and ASTER. The RBE applied to Landsat 8 data which has high radiometric resolution provided better accuracy compared to other satellite data in terms of correlation coefficient (R=0.89 and 0.80), coefficient of determination (R^2=0.81 and 0.66) and Root Mean Square Error (RMSE=1.39m and 2.09m) from images collected on 31 January, 2014 and 4 March, 2014 respectively. The multispectral algorithm originally proposed by Clark et al., (1987, 1988) used only visible bands to estimate depth. Since the Clark et al., (1987and1988) were using a linear regression between multispectral bands and in-situ depth, here onwards depth estimation algorithm using multi-spectral bands from visible region from electromagnetic spectrum is called as Multiple-band Linear Regression (MLR). Multispectral bands are account for the varying degree of attenuation coefficient by addressing the heterogeneity of bottom types. This study proposes a new band combination to include Near Infra Red (NIR) band for depth estimation. The method to estimate depth using new band combination with visible and NIR band is hereafter called as MLR-NIR. The MLR and MLR-NIR were tested with the same data sets and observed that the results significantly improved by the proposed MLR-NIR. The depth estimation results derived from Landsat 8 data collected on 12 November, 2013, 31 January, 2014 and 4 March, 2014 by applying MLR-NIR shown better correlation coefficient (R=0.95, 0.95 and 0.90), coefficient of determination (R^2=0.91, 0.91 and 0.83) and RMSE (1.53m, 0.83 m and 1.23m) as compared with MLR. The depth estimates derived from Landsat 8 data were used to investigate the reduction in accuracy due to turbidity has been carried out. The results indicate that NDWI (Normalized Difference Water Index) impacts the accuracy of depth estimates but not very significantly.

1. Introduction

Determination of water depths in coastal zone is a common requirement for any coastal engineering work and research related to coastal zone. The highly dynamic nature of coastal zone leads to frequent change in water depths that are required to be monitored at periodic intervals.

In order to better manage and protect the coastal zone, it is necessary to comprehend coastal zone conditions affected by shallow water depth. Mapping shallow water depth from ships by sonar is a quite an expensive task. Many shallow water areas are not accessible by hydrographic ships due to rocks, coral reefs or simply due to inaccessibility by boats due to

shallow depth of the water. Airborne Light Detection and Ranging (LIDaR) can provide complete and accurate bathymetric measurements in shallow areas, but availability of this technology is currently limited and also involves significant cost. Thus, there is a need for an alternative method to estimate multi-temporal depth variations. In order to supplement field based approaches, a number of passive RS methods have been proposed by many authors (Brown et al., 1971, Lyzenga, 1978, Tripathi et al., 2002, Philpot, 1989 and Benny and Dawson, 1983). Several workers (e.g. Stoffle and Halmo, 1991, Stumpf et al., 2003, Lyzenga et al., 2006 and Pacheco et al., 2015) successfully demonstrated the use of satellite RS data for determination of depth in coastal waters. Multiple band techniques have been commonly used for depth estimation from shallow water (e.g. Fonstad and Marcus, 2005 and Ceyhun, Yalçýn 2010) but these multiple band techniques depend upon large amounts of ground truth data and a fine enough resolution to discriminate bottom types. There are conflicting opinions expressed over the suitability of spectral wavelength bands for water depth estimation. Kumar et al., (1997) used 0.77–0.80 µm wavelength for depth measurements in an estuary. Warne, (1972) adopted 0.5–0.6 µm range and Yi and Li (1988) also adopted 0.47–0.54 µm band for measuring water depth. George (1997) found 0.746–0.759 µm range to be more suitable compared to wavelength bands. Manessa et al., (2014), also observed that NIR band (0.77-0.89 µm) is close to the visible spectrum and still sensitive to bottom reflectance. Ibrahim et al., (1990), used 0.5-0.6 µm (band 4) of Landsat 3 MSS to estimate depth by correlating the intensity of pixels and depth for Peg island in Malaysia. The shallowest areas show bottom reflectance in 0.77-0.90 µm range but deeper areas (greater than 15 m) show bottom reflectance only in 0.45-0.52 µm range (Jupp et al., 1988). In the last two decades, several researches on optical RS were focused on formulating shallow water depth estimation algorithms. Although several algorithms have already been discussed, main purpose of this study is to evaluate the efficacy of some of the algorithms to recently available high radiometric and spatial resolution RS data. Further, modification and improvements had made to the methods to obtain better results. Algorithms dealing with depth estimation are mainly categorized in to single and multiple bands in terms of number of spectral band used. This study aims at evaluating about both single band and multispectral bands approaches have proposed by Stoffle and Halmo, (1991) and Clark et al., (1987 and 1988). This study also proposes the new RBE method to estimate depth from single band without the need of *in-situ* depth and also proposes improved depth estimation using Clark method with new band combination. Further, these proposed methods have been validated various kinds of radiometric, spatial and temporal resolution data sets such as Landat 7, Landsat 8 and ASTER.

2. Algorithms for Estimating Water Depth

The SLR method proposed by Stoffle and Halmo, (1991) and MLR method proposed by Clark et al., (1987) discussed below are most commonly used algorithms for bathymetric estimation from shallow water region.

2.1 Single-Band Linear Regression (SLR)

The Stoffle and Halmo, (1991) have proposed algorithm that have been used to estimate depth from single band. The depth is estimated based on equation below:

$$h = -1/2kX(\lambda)_i + 1/2k(logV_0)$$

Equation 1

Where, h is estimated is depth; $X(\lambda)_i$ is corrected transformed radiance which is linearly related to the depth, k is water attenuation coefficient. V_0 is sensitivity factor related to solar irradiance at the surface, the bottom reflectance, atmospheric transmission, and sensor equipment (Gholamalifard et al., 2013). The equation (1) takes the form of *depth = slope* $X(\lambda)_i$ *+ constant*. The line in this equation describes the best fit of a simple linear regression using known depth measurements as the dependent variable and the transformed radiance $(X(\lambda)_i)$ as the independent variable. The slope of this line is related to the water attenuation coefficient such that slope is $-1/2k$, and the constant value is given by $1/2k\ (logV_0)$. The SLR method assumes a constant attenuation coefficient and homogeneous bottom type in the overall study area and also assumes the transformed radiance of single band corresponds directly to water depth. The limitation of this method is that it needs *in-situ* depth to compute linear relationship and estimate depth. In order to address this problem study proposes the RBE method. The RBE method directly applied to the transformed single band without need to consider about the radiative transfer of light in the sea water. The attenuation coefficient in a particular single band is calculated using SLR algorithm to understand the radiative transfer of light for a particular band. RBE is suggested to be used as an extension to SLR method to estimate depth from multi-temporal satellite imageries. In RBE, a single band is selected in order to derive better depth estimation and this particular band of other satellite imageries is used to

estimate depth. Only one reference data (maximum depth value) which is estimated by SLR method has to be used as input for the RBE. The highest value for depth derived by SLR method is considered as constant for all multi-temporal images. Apart from that, the constant maximum value can also be assigned arbitrarily in case *in-situ* depth is unavailable to apply RBE. A conversion factor is calculated by the following equation.

$$Conversion\ factor = Dmax/C$$

Equation 2

Where, *Dmax* is the maximum depth value derived by SLR method, which is considered as constant for other satellite imageries. *C* is unique cell values in a single transformed band. The conversion factor is applied to the transformed band and depth is estimated.

2.2 Multiple-band Linear Regression (MLR)

Several authors (Clark et al., 1988, Hamilton et al., 1993, Kanno and Tanaka, 2012) recognized multiple regression analysis would provide good depth estimation using multiple bands over shallow water region. Originally, Clark et al., (1987) proposed a multiple regression analysis between *in-situ* depth and multispectral bands to estimate coefficients. Further, these coefficients have been used to estimate the depth. This method addresses the heterogeneity of the bottom type by utilizing all the visible bands. This algorithm attempts to isolate water attenuation and hence depth using a combinations of spectral bands. MLR utilizes multispectral band, so that it accounts for varying attenuation coefficients for different bottom types as it calculates water depth (Van Hengel and Spitzer, 1991). The equation to estimate depth is following:

$$h = \beta_0 + \beta_1 X(\lambda)_1 + \beta_2 X(\lambda)_2 + \cdots + \beta_n X(\lambda)_i$$

Equation 3

Where h is the estimated depth, β_0, β_1, β_2... β_n are derived constants and $X(\lambda)_1$, $X(\lambda)_2$,...$X(\lambda)_i$ are the log transformed atmospheric, water surface and water column corrected radiance values of multiple bands. The band combination using in the multispectral methods have significant impact of the accuracy of the results.

There is a lack of agreement amongst researchers about the right band combination for better depth estimation. Many authors (Lyzenga et al., 2006 and Kanno and Tanaka, 2012), used NIR band for atmospheric and water column corrections. However, this leads to significant errors in the shallow depth region due to reflectance from the bottom in NIR band (Manessa et al., 2014). Therefore, this study proposes a new band combination that includes visible NIR band for depth estimation.

3. Materials and Methods

3.1. Study Area

The study area shown in Figure 1 is located off Ratnagiri along the Arabian Sea coast with maximum depth of 11m. Geographically it stretches 73°16'30"E - 73°18'00"E 16°57'00"N - 16°59'30"N with 5 Km long coastal zone, that includes 70% of sandy beach and an estuary of Kajali River. Along the study area, the coast is exposed to seasonally reversing monsoon winds, with winds from the southwest (SW) direction during the SW (summer) monsoon period (June to September) and from the northeast (NE) during the NE (winter) monsoon period (October to January). Tides in the region are mixed and are predominately semi-diurnal and the annual rainfall of the region is around 3m. The near-shore depth is highly dynamic due to sediment discharge from the Kajali River and seasonal climate changes. The relative sea level rise of the area is 0.9mm/year (Chouhan et al., 2003) is comparatively very less than global average of sea level rising 3mm/year (Holgate and Woodworth, 2004).

3.2 Data used

Several satellite images were used from multi-sources with various radiometric and spatial resolutions. Landsat 7 data available at 30 meter spatial resolution and radiometric quantization at 8 bit dynamic range. Recently, Landsat 8 data are freely available which has higher radiometric resolution quantized over a 12-bit dynamic range (This translates into 4096 potential DN value range in an image compared with only 256 DN value range in previous 8-bit instruments.). Even though ASTER data has the radiometric resolution of 8 bit, it provides the spatial resolution of 15 meter. Two field surveys were carried out to collect depth data from the study area. These *in-situ* depths were used for calibration and evaluation of the depth estimation. Detailed description of the characteristics of data used is shown in the Table 1.

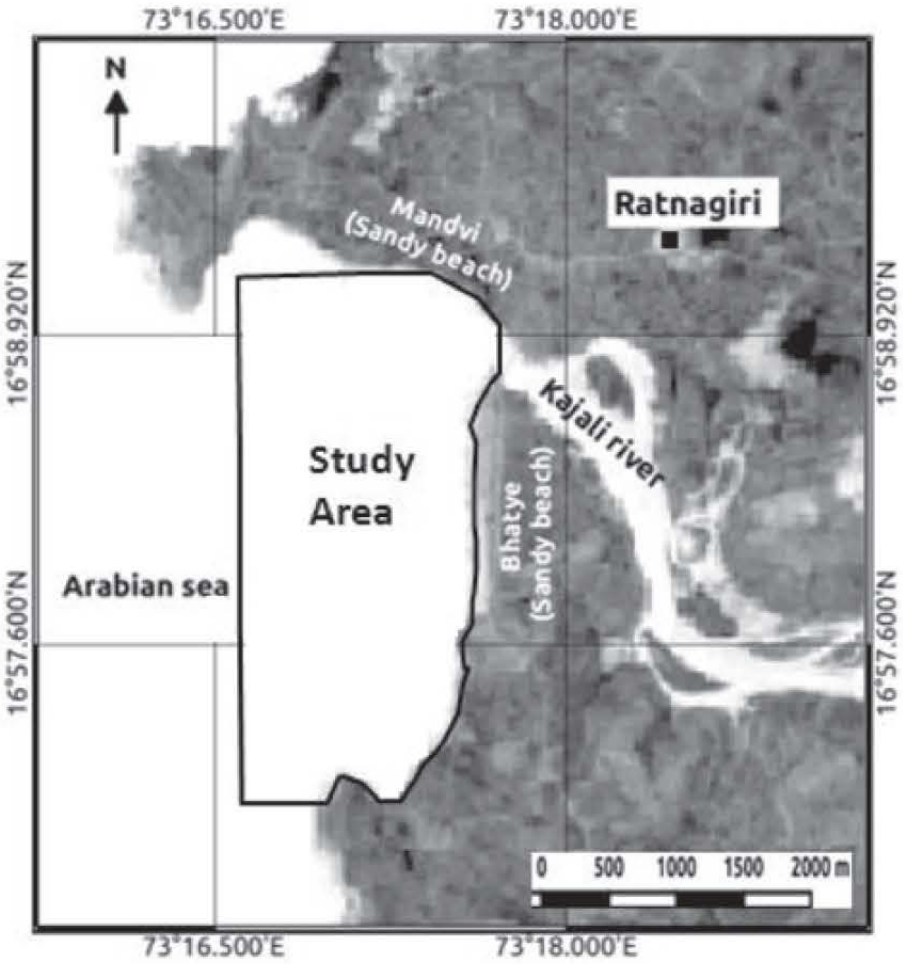

Figure 1: Study area

Table 1: Characteristics of data used for this study

Date	Source	Tide (m)	Resolution (m)
09-05-2012	Landsat ETM	1.15	30
27 May, 2012	*In-situ* depth	1.53-2.3	10
30 March, 2003	Landsat ETM	2	30
2003	NHO chart (1:60,000)	2.3	30
08 May, 2000	Landsat (ETM)	1.36	30
12 November, 2013	Landsat 8	1.25	30
31 January, 2014	Landsat 8	2.40	30
04 March, 2014	Landsat 8	1.66	30
17 November, 2013	*In-situ* depth	2.24-2.35-2.16	7
10 December, 2012	ASTER	1.03	15
16 January, 2003	ASTER	1.8	15

3.3 Pre-Processing

Several pre-processing procedure have been carried out prior to the depth estimation. Pre-processing procedures are same for SLR method, RBE and MLR-NIR.

3.3.1 Tide correction of in-situ depth

Since the satellite images and *in-situ* depth were collected at different time and tide conditions, tide correction need be applied to the *in-situ* depth to tide at the time of the corresponding image capture.

Tide data collected by tide gauges operated by National Institute of Oceanography (NIO) were used for applying corrections. The tide at the time of satellite image capturing is unique but in case of field surveys, start at a time with one tide and ends at other time with different tide. Therefore, the variation in the tide height of *in-situ* depth is also addressed by tide correction. For instance, The tide of *in-situ* depth collected on 27 May, 2012 is vary from 1.53m to 2.3m, therefore the tide of the *in-situ* depth is corrected to the tide of the image (1.15m) collected on 9 May, 2012 (Landsat 7). All the in-situ depths collected are tide corrected according to the tide of the time of satellite image is used to estimate depth.

3.3.2 Radiance conversion

All the satellite data were already geometrically and radiometrically calibrated. Digital Numbers (DN) were converted to physical units of band averaged spectral units (Watts/(m^2×srad×μm)). Equations for radiance ($L\lambda$) conversion for Landsat 7, Landsat 8 and ASTER are explained below. For Landsat 7 image,

$$L(\lambda) = (L_{max} - L_{min}/255) \times DN + L_{min}$$

Equation 4

Where, L_{min} is the minimum radiance, L_{max} is the maximum radiance and *DN* is the digital number of a particular band. For Landsat 8 the equation used to convert to radiance is:

$$L(\lambda) = ML \times Qcal + AL$$

Equation 5

Where, *ML* is Band-specific multiplicative rescaling factor (RADIANCE_MULT_BAND_x, where x is the band number), *AL* is Band-specific additive rescaling factor (RADIANCE_ADD_BAND_x, where x is the band number), Qcal is Quantized and calibrated standard product pixel values (DN). In case of ASTER, Radiance is calculated as shown in the equation (Lillesand et al., 2004) below:

$$L(\lambda) = (DN - 1) \times Unit\ conversion\ coefficient$$

Equation 6

3.3.3 Lyzenga's correction

The radiance observed by a satellite sensor on shallow water basically consist of four components, namely, atmospheric scattering component, surface reflection component, in-water volume scattering component, and bottom reflection component (Kanno and Tanaka, 2012). Many authors (Baban, 1993, Muslim and Foody, 2008) have also suggested a component of bottom reflectance in shallow water images. Bottom reflectance is transformed to depth values after removing other three components (atmospheric scattering component, surface reflection component, in-water volume scattering component) successfully. There are two very important procedures that must be undertaken prior to Lyzenga's correction (Lyzenga, 1981). The first step is to distinguish water from the land. The ratio of green and short wave infrared bands was computed and ratio of greater than 1 was classified as water and less than 1 as land. Water region separated by masking land area has been used for further analysis. The second pre-processing procedure involves correction of the imagery to remove random noise and stripping. Since the methods are sensitive to random noise and striping, image smoothing with a low-pass 3×3 filter has been carried out. In Lyzenga's correction method sea-surface scattering or atmospheric scattering are implicitly assumed to be homogeneous over the target area. In case of deep water, the observed spectral radiance (L(λ)) at infinite depth *(h), (L(λ∞)* is assumed not to include bottom reflectance, such that the water depth only consists of information related to external reflection from the water surface and atmospheric scattering. Subsequently, the effects of atmospheric scattering, surface reflection and in-water volume scattering can be eliminated by subtracting the average radiance of the deep water $L(\lambda \infty)$.

$$C(\lambda)_i = (L(\lambda)_i - L(\lambda\infty)_i)$$

Equation 7

Where, $C(\lambda)_i$ is the corrected radiance, $L(\lambda\infty)_i$ represents the averaged radiance of deep water and subtracted standard deviation of radiance for $_i{}^{th}$ band. Whereas pixels corresponding to shallow waters are of current interest, deep water pixels can be considered to corresponding to an infinite depth and discarded. The deep water pixels have a low overall reflectance than the shallow water pixels, and hence easy to separate. Subsequently the corrected radiance values $(C(\lambda)_i)$ were calculated from blue, green, red and NIR bands separately as mentioned in equation (7). The steps for Lyzenga's correction were shown in the Figure 2.

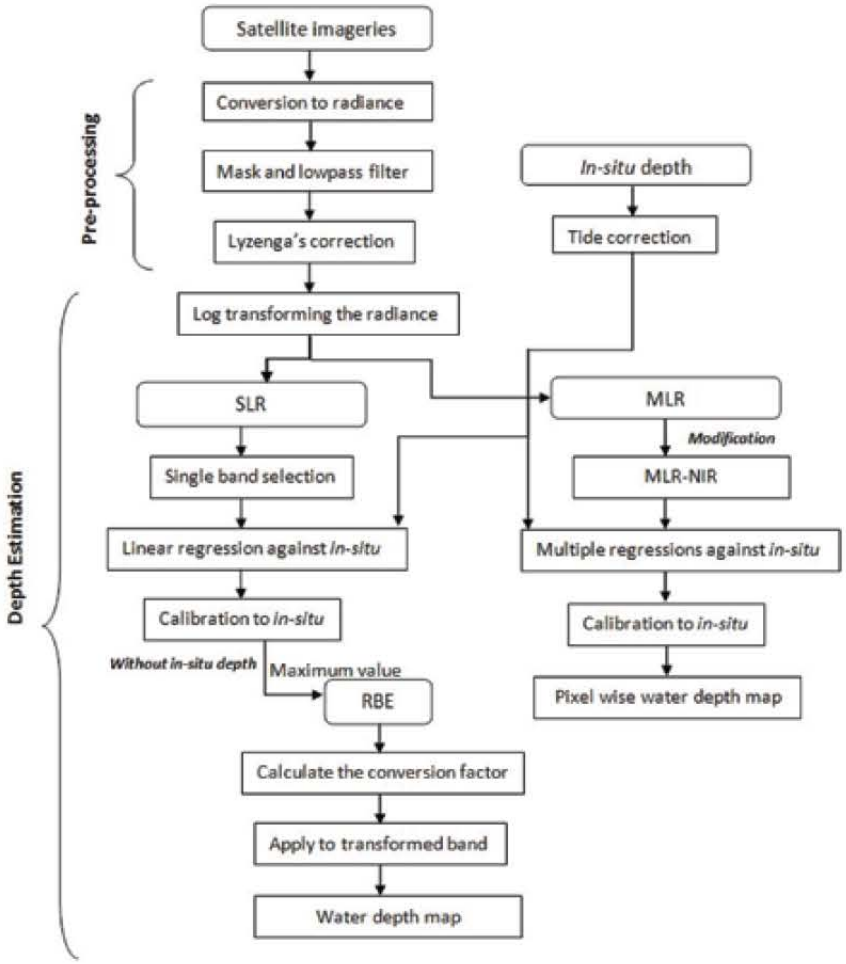

Figure 2: Flow chart of the proposed methods

3.4 Depth Estimation

After atmosphere, water surface and water column correction applied to the bands, the radiance is logarithmically transformed to investigate relationship between radiance and depth. The equation for the log transformed radiance can be denoted as:

$$X(\lambda)_i = log(C(\lambda)_i)$$

Equation 8

Where, $X(\lambda)_i$ is log transformed radiance values of i^{th} band.

3.4.1 Single Linear Regression (SLR) and Radiance Based Estimation (RBE)

A single band was selected from particular satellite imagery to apply SLR method and RBE. In empirical modeling, the relationship between the remotely sensed radiance of a water body and the depth at sampled locations is established without considering how light is transmitted in water (Gao, 2009). To select a single band for applying algorithms, correlation coefficient is calculated by simple linear regression between the transformed bands and *in-situ* depth measurement value. The transformed band is considered as independent variable ($X(\lambda)_i$) and depth (y) as a dependent variable as shown in equation below:

$$y = a + bX(\lambda)_i$$

Equation 9

Any single band that provides better correlation coefficient as compared to other bands is selected for depth estimation. The maximum depth value derived from the SLR method over the study area is arbitrarily chosen as an input value for the RBE method to estimate depth when there is no corresponding *in-situ* depth available. It has been observed that in all the multi-temporal data, NIR (0.77-0.90 µm) band provides better correlation compare to other bands in the study area.

In lighted the above observations, NIR band was chosen to apply SLR method and RBE for all the satellite imageries. The workflow of RBE method is explained in detail below with an example of Landsat 7 data. First of all, RBE is applied to Landsat 7 image 30 March, 2003 and, subsequently, reliability of the method was tested with other data set too. In addition to SLR method assumptions, RBE method also assumes that the maximum depth value for all temporal data set is assigned as constant. To apply RBE method to an imagery only one *in-situ* depth value as maximum value is necessary. Here, maximum depth value is derived from 9 May, 2012 image (11m) by applying SLR is assigned as constant for all images of other dates in order to apply RBE.

Tide correction will be applied to the single maximum depth value with respect to the tide of image capture. The tide height during Landsat 7 image acquisition (30 March, 2003) was 2.01m. Since the tide height of image collected from 9 May 2012 depth is 1.15m, the maximum depth value will be changed to 11.86m after adding 0.86m to the constant maximum depth (11m) in order to correct the tide rise and fall. So the maximum depth value in case of 30 March, 2003 image is changed to 11.86m. The transformed radiance (Figure 3B) has 68 unique cell values; hence the maximum depth 11.86m is divided by 68 to derive conversion factor (0.174411765). The maximum value in the transformed radiance (Figure 3B) is 2.36.

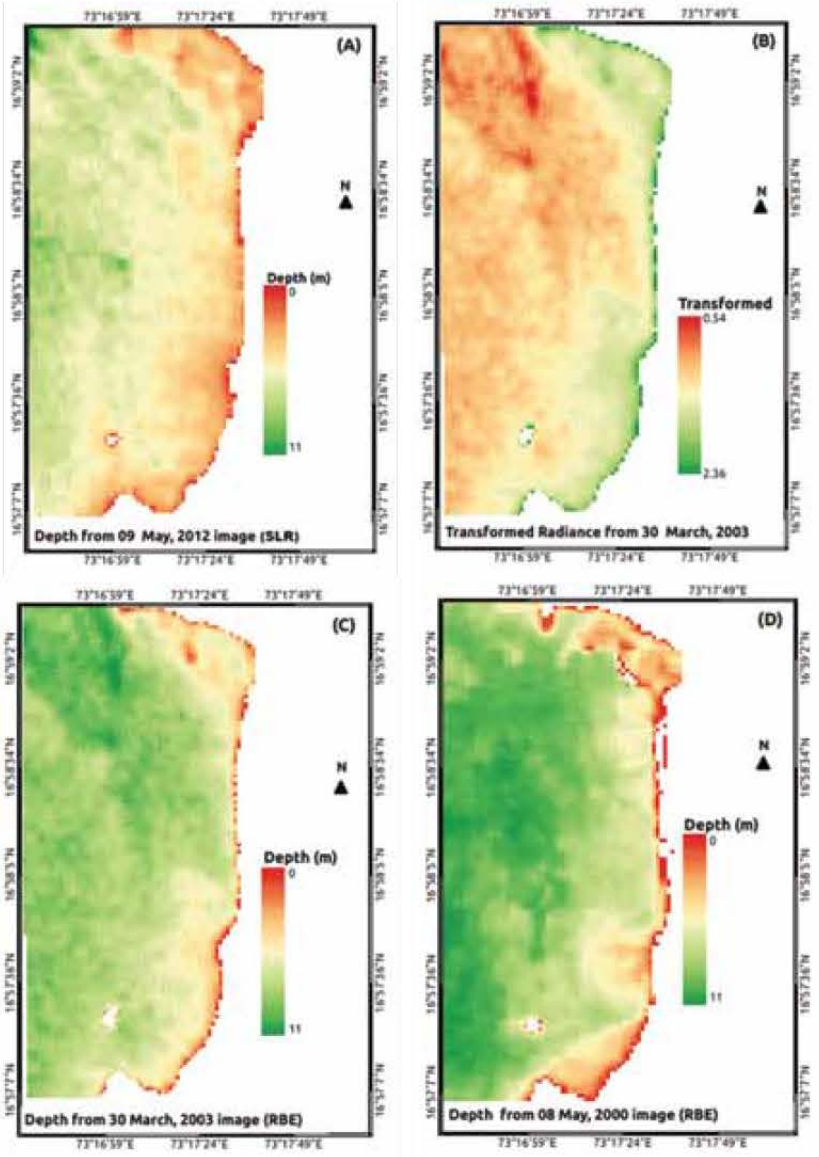

Figure 3: Depth map by SLR method from Landsat 7, (A) depth for 09 May, 2012, (B) Transformed radiance of NIR band of 30 March, 2003, (C) depth for 30 March, 2003 and (D) depth for 08 May, 2000

The cells are having unique value as 2.36 in the transformed radiance are changed to 0.174411765m depth. Subsequently all the cell values are transformed to depth by adding conversion factor incrementally to the transformed radiance. Eventually, the cells having unique value as 0.54 in the transformed radiance has changed to 11.86m depth. Hence, 68 classes of unique depth values are derived by the RBE method (Figure 3C). The same way, depth was estimated from other data sets such as Landsat 8 and ASTER. The count of different cell values (denoted by C in equation 2) will vary according to the DN value ranges of the data.

3.4.2 Multiple-band linear regression with new band combination (MLR-NIR)

Several authors have been used different band combinations to estimate depth. But in this study we propose a new combination including both visible and NIR spectral bands. As described in the equation (3) multiple linear regressions were carried out between the log transformed visible and NIR bands and *in-situ* depth. Where, log transformed bands ($X(\lambda)_1, X(\lambda)_2, \ldots X(\lambda)_i$) are taken as independent variable and *in-situ* depth has taken as dependant variable. The coefficients ($\beta_0, \beta_1, \beta_2 \ldots \beta_n$) derived from multiple linear regressions have been used to estimate the depth for all pixels. The workflow is explained in Figure 2. The new combination of bands was tested with all available data sets with corresponding *in-situ* depth. If the corresponding *in-situ* depth was not available, *in-situ* depth collected close to the image capture date was used for multiple regression and calibration. The details of the *in-situ* depth and satellite imageries are shown in Table 1. From 2000 to 2014, various multi-temporal and multi source data sets were used to estimate the depth along Ratnagiri coast. Landsat 7, Landsat 8 and ASTER data were used to estimate depth and used to compare the behavior of the algorithms in various spatial and radiometric resolutions. The water over the study area is not very clear, and also slightly turbid due to the sedimentation from the Kajali River. Therefore, in this study we evaluated different methods which utilize single band as well as the multi-spectral bands for estimating depth. The comparative evaluation mainly focused on two objectives, namely multi-temporal depth estimation from single band even without *in-situ* depth and, secondly, on investigating appropriate band combination of multi-spectral bands to estimate depth with better accuracy. Since the single band algorithms and multispectral band algorithms treated separately in this study, the accuracy, and error related to the results obtained by these methods are also discussed separately. Implementation of all the algorithms for atmospheric correction and depth estimation carried out in Open Source GRASS GIS (http://grass.osgeo.org/).

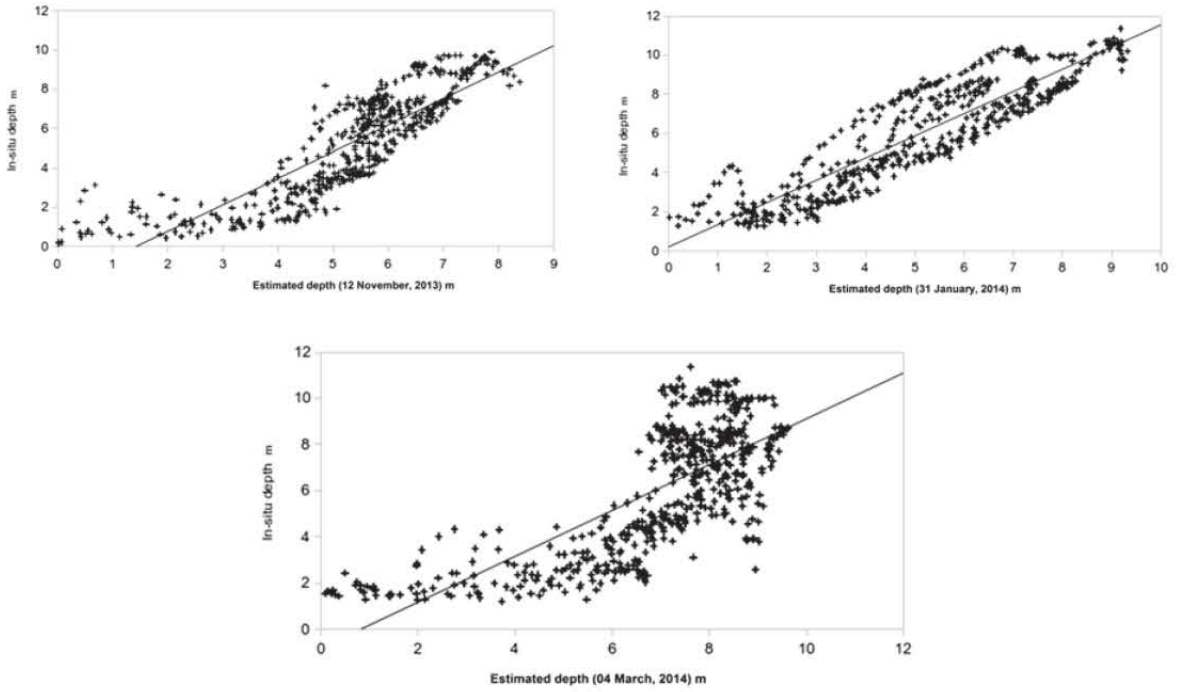

Figure 4: Bivariate scatter plots between depth estimated by single band of Landsat 8 and *in-situ*

4. Results

SLR method was applied to 9 May, 2012 (Landsat 7) image, 12 November, 2013 image (Landsat 8) and 10 December, 2012 (ASTER) are calibrated and evaluated using *in-situ* depth collected on 27 May, 2012, 17 November, 2013 and 17 November, 2013 respectively. The evaluation of the results derived by RBE is carried out with *in-situ* depth collected closer to the image acquisition date. In the case of 8 May, 2000 and 30 March, 2003 (Landsat 7) and 16 January, 2003 (ASTER) images, NHO chart data surveyed on 2003 was used, In case of 31 January, 2014, 4 March, 2014 (Landsat 8) and 10 December, 2012 (ASTER) *in-situ* data collected on 17 November, 2013 was used. The comparison of estimation results of all the satellite imageries used in this study carried out by correlation coefficient (R), coefficient of determination (R^2) and RMSE. All these parameters used to evaluate the accuracy of results shows that depth estimation derived from Landsat 8 data was providing better accuracy than other satellite imageries (Table 2). Landsat 8 data was collected on 31 January, 2014 and 04 March, 2014 were providing correlation coefficient (R=0.89, 0.80), coefficient of determination (R^2=0.81, 0.66) and RMSE (1.39m, 2.09m) respectively. High radiometric resolution of Landsat 8 data provides better depth estimation as compared to other data sets. Even though ASTER data has high spatial resolution than Landsat 8, it was not effective in providing comparable results of Landsat 8 data. More significantly, RBE proposed in this study shows a unique estimation capability for all the data sets. Since RBE directly converts transformed radiance to depth, it is very sensitive to correction methods. If the correction method is able to remove all the noises obtained from the atmosphere, water surface and water column reflectance, then the RBE could provide far better results than occurred. Unfortunately, till now there is no algorithm could remove completely the noises from satellite imageries. The second method (MLR-NIR) was used to estimate depth from all available satellite imageries. In case of Landsat 7 four bands (0.45-0.90μm), in case of Landsat 8 five bands (0.43-0.88μm) and in case of ASTER three bands (0.52-0.86μm) were used. The results derived by MLR-NIR were compared and evaluated with the results derived from MLR. Evaluation carried out in terms of correlation coefficient, coefficient of determination and RMSE. The results show that depth estimation by MLR-NIR has provided better accuracy than the MLR (Table 3).

Table 2: The estimated multi-temporal depth from various data sets by the proposed single band method

Data source	Date	Method	R	R^2	RMSE(m)
Landsat 7	09 May, 2012	SLR	0.67	0.46	2.14
	30 March, 2003	RBE	0.63	0.41	2.83
	8 May, 2000	RBE	0.74	0.56	2.88
Landsat 8	12 November, 2013	SLR	0.85	0.74	1.46
	31 January, 2014	RBE	0.89	0.81	1.39
	04 March, 2014	RBE	0.80	0.66	2.09
ASTER	10 December, 2012	SLR	0.70	0.50	2.10
	16 January, 2003	RBE	0.57	0.34	2.38

Table 3: Comparison of accuracy of depth estimated from different combinations of multispectral bands (MLR and MLR-NIR)

	Date	MLR			MLR-NIR		
		R	R^2	RMSE (m)	R	R^2	RMSE (m)
Landsat 7	8 May, 2000	0.80	0.66	1.64	0.82	0.69	1.57
	30 March, 2003	0.65	0.44	2.44	0.77	0.61	2.07
	09 May, 2012	0.53	0.30	1.77	0.68	0.48	1.53
Landsat 8	12 November, 2013	0.91	0.84	1.77	0.95	0.91	1.53
	31 January, 2014	0.91	0.84	1.12	0.95	0.91	0.83
	04 March, 2014	0.85	0.74	1.43	0.90	0.83	1.23
ASTER	16 January, 2003	0.76	0.59	1.90	0.78	0.62	1.86
	10 December, 2012	0.69	0.50	1.75	0.76	0.60	1.56

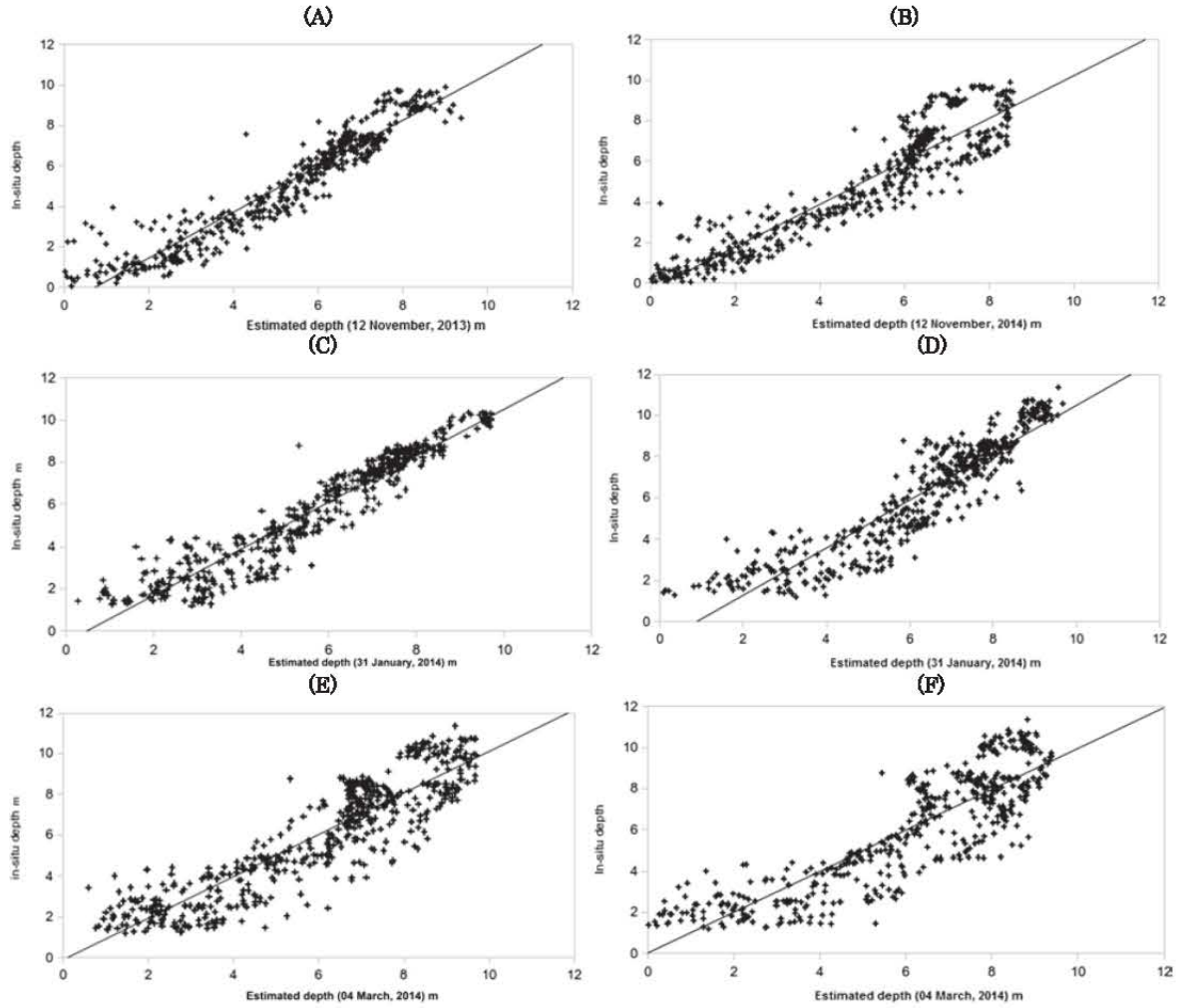

Figure 5: Bivariate scatter plot between depths estimated from Landsat 8 and *in-situ* depth. The MLR-NIR (A, C and E) and MLR (B, D and F) are shown respectively

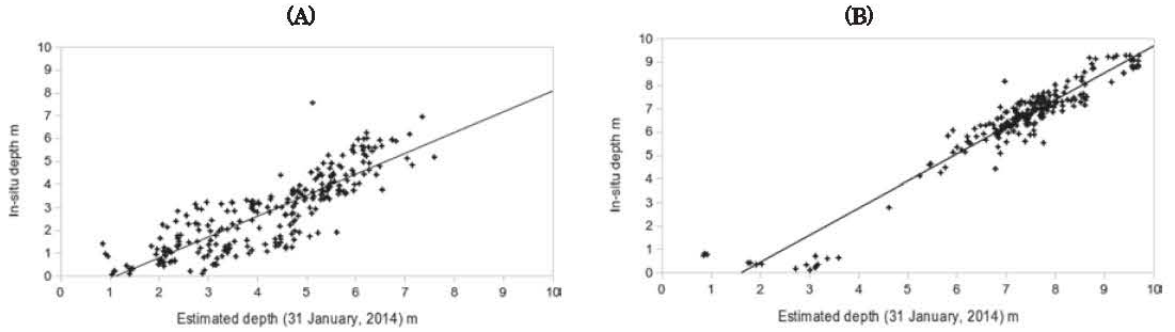

Figure 6: Bivariate scatter plot between estimated depth using Landsat 8 and *in-situ* depth at high turbid (A) and low turbid (B) region

Especially, in Landsat 8 data (12 November, 2013, 31 January, 2014 and 04 March, 2014) provides better accuracy results in terms of correlation coefficient (R=0.95, 0.95, 0.90), coefficient of determination (R^2=0.91, 0.91, 0.83) and RMSE (0.83m, 1.23m) respectively. The Figure 5 shows the bivariate scatter plot between depth estimates and *in-situ* depth derived from Landsat 8.

Table 4: Comparison of accuracy of depth estimated from Landsat 8 data in terms of turbidity

Date of data	Methods	NDWI	R	R^2	RMSE (m)
12 November, 2013	RBE	Low turbid	0.88	0.78	1.21
		High turbid	0.82	0.67	1.50
	MLR-NIR	Low turbid	0.97	0.94	0.85
		High turbid	0.90	0.81	0.90
31 January, 2014	RBE	Low turbid	0.82	0.68	1.27
		High turbid	0.77	0.60	1.36
	MLR-NIR	Low turbid	0.95	0.91	0.97
		High turbid	0.84	0.71	1.65
04 March, 2014	RBE	Low turbid	0.77	0.59	2.70
		High turbid	0.65	0.43	2.82
	MLR-NIR	Low turbid	0.93	0.86	1.48
		High turbid	0.85	0.72	1.85

In Figure 5 A, C and E show the bivariate scatter plot of depth estimates derived from MLR-NIR and B, D and F are from MLR. Bivariate scatter plots clearly demonstrate that the proposed new band combination MLR-NIR is better than the other. The new modified band combination shows significant increase in the accuracy irrespective the satellite imageries are used. Observed good accuracy in Landsat 8 was due to the availability of new coastal aerosol (0.43-0.45µm) band. The accuracy and error evaluation tests were also carried out to estimate accuracy and error obtained due to turbidity in depth estimate derived by both single band and multi-band methods from Landsat 8 data. The study area was divided into two sections based on Normalized Difference Water Index (NDWI). The NDWI originally introduced by Rogers and Kearney (2004) to envisage coastal marsh, where, lower NDWI value denote high turbidity and higher NDWI values indicate relatively low turbidity. The evaluation tests confirm that the accuracy of the depth estimates at low turbid area is higher than the high turbid region. Table 4 summarizes the evaluation results carried out by using R, R^2 and RMSE. The RMSE values indicate that error associated the depth estimates increases in high turbid region. The estimated depth results at high turbid region and low turbid region are compared using bivariate scatter plot in Figure 6. Low turbid region shows stronger linear relationship between estimated depth and *in-situ* depth than high turbid region. Figure 6 demonstrate the scatter plot of estimated depth derived from Landsat 8 data (31 January, 2014) by MLR-NIR method and *in-situ* depth. Other data summarized in the Table 4 are also showing the similar trend. However, the turbidity due to wave action along the coast or dynamic sediment discharge near estuary potential to reduce the accuracy of the depth estimation.

5. Discussion and Conclusions

The two different methods RBE and MLR-NIR proposed in this study were capable to estimate water depth in different situations. The RBE single band method is an extension to the SLR method. In the single band method, attenuation coefficient assumed to be constant in the study area, to consider otherwise would have required more ground truth knowledge about bottom type that are often not available. The attenuation of light in a particular band is estimated by using SLR method and multi-temporal images of same band was used for investigating bathymetric changes. RBE method depends only on radiance value of transformed band. The limitation of single band method is that, it does not address the issues of heterogeneity occurred due to difference in bottom type and water quality. However, the advantage of this method is that it is feasible even in situations where *in-situ* data is lacking. Results derived by RBE from various data sets with different spatial and radiometric resolution were evaluated by *in-situ* depth and observed good accuracy in quantitative terms. Landsat 8 data with high radiometric resolution was provides better results using RBE. Further, an attempt has also been carried out to comprehend the reduced accuracy of the RBE due to turbidity. Results show that turbidity affects the attenuation of the light and affects accuracy of derived depth but does not significantly degrade the estimation. The MLR-NIR is the second method proposed by this study is a modification of multi-spectral band combination. The multispectral band method accounts for variations in attenuation

coefficients depending on wavelength used, sea bottom types, and water column properties. Since NIR wave length is capable of capturing the bottom reflectance in shallow water, a new multispectral band combination including NIR band has been proposed and evaluated. Limitation of this method is that a good amount of in-situ depth is needed in order to estimate the coefficients for calibration. However, MLR-NIR provides good estimates of depth in all the available satellite imageries. A comparative study was carried out between MLR and MLR-NIR. The results show that the MLR-NIR provides better depth estimates as evident from improved correlation coefficient, coefficient of determination and RMSE. The results indicate that the newly proposed method (RBE) can be applied to any other optical RS imagery band which contains the bottom reflectance to estimate depth. It is also observed that the inclusion of NIR band for the depth estimation from multispectral bands potentially increases the accuracy of the results. The accuracy of the result could be increased by establishing an algorithm to focus on better atmospheric correction, without losing the depth information. The complexity of coastal waters, as well as the atmosphere above, requires more robust algorithms capable of handling bathymetric modeling. Further investigation is necessary for better discrimination of bottom reflectance from top-of-atmosphere radiance and signal carrying information of materials suspended in seawater. The algorithm could be refined by new correction method using short-wave Infrared band (1.57-1.65 μm) of Landsat 8.

Acknowledgement

This work was supported by Japanese Government (Monbukagakusho: MEXT) Scholarship awarded to the first author. We express our sincere thanks to MEXT and Osaka City University for supporting this research. We are also grateful to National Institute of Oceanography (NIO), Goa, India for supporting *in-situ* depth data collection. The authors would like to express a sincere gratitude to Dr. Ariyo Kanno, Yamaguchi University, Japan for his valuable comments on shallow water depth estimation. We also sincerely thank Mr. Jubin Thomas, NIO, Regional Center Mumbai, India for providing tide data.

References

Baban, S. M. J., 1993, The Evaluation of Different Algorithms for Bathymetric Charting of Lakes using Landsat Imagery. *International Journal of Remote Sensing*, 14, 2263–73.

Benny, A. H. and Dawson, G. J., 1983, Satellite Imagery as an Aid to Bathymetric Charting in the Red Sea. *The Cartographic Journal,* 20(1), 5–16.

Brown, W. L., Polcyn, F. C. and Stewart, S. R, 1971, A Method for Calculating Water Depth, Attenuation Coefficients and Bottom Reflectance Characteristics in Proceedings. *Seventh International Symposium on Remote Sensing of the Environment*, 663-680.

Ceyhun, O. and Yalçın, A., 2010, Remote Sensing of Water Depths in Shallow Waters Via Artificial Neural Networks. *Estuar. Coast. Shelf Sci.,* 89, 89–96.

Chauhan, O. S., Unnikrishnan, A. S, Messeses, A. A. A., Jagtap, T. G., Sumeethi, J. and Furtado, R., 2003, Vulnerable Areas and Adaptation Measures for Sea Level Rise along the Coast of India. Workshops on Water Resources. *Coastal Zone and Human Health,* 83-94.

Clark, R. K., Fay, T. H. and Walker, C. L., 1987, Bathymetry Calculations with Landsat-4-TM Imagery under a Generalized Ratio Assumption. *Appl. Opt.*, 26, 19, 4036–4038.

Clark, R. N., Faye, T. H. and Walker, C. L., 1988, Bathymetry using Thematic Mapper Imagery. *Proc. SPIE, Ocean Optics IX*; doi:10.1117/12.945728, 925, 229-231.

Fonstad, M. A. and Marcus, W. A., 2005, Remote Sensing of Stream Depths with Hydraulically Assisted Bathymetry (HAB) Models. *Geomorphology*, 72, 320–339.

Gao, J., 2009, Bathymetric Mapping by Means of Remote Sensing Methods, Accuracy And Limitations. *Progress in Physical Geography*, 33(1), 103–116

George, D. G., 1997, Bathymetric Mapping using a Compact Airborne Spectrographic Imager (CASI). *International Journal of Remote Sensing*, 18, 2067–2071.

Gholamalifard, M., Kutser, T., Esmaili, Sari A., Abkar, A. and Naimi, B., 2013, Remotely Sensed Empirical Modeling of Bathymetry in the Southeastern Caspian Sea. *Remote Sensing*, 5, 2746-2762.

Gholamalifard, M., Esmaili Sari, A., Abkar, A. and Naimi, B., 2013, Bathymetric Modeling from Satellite Imagery via Single Band Algorithm (SBA) and Principal Components Analysis (PCA) in Southern Caspian Sea. *International Journal of Environmental Research*, 7(4), 877-886.

Hamilton, M. K., Davis, C. O., 1993, Estimating chlorophyll content and bathymetry of Lake Tahoe using AVIRIS data. *Remote Sensing of Environment*, 44(2-3), 217-230.

Holgate, S. J. and Woodworth, P. L., 2004, Evidence for Enhanced Coastal Sea Level Rise during the 1990s. *Geophysical Research Letters*, 31, L07305, doi:10.1029/2004GL019626.

Ibrahim, M., and Cracknell, A. P., 1990, Bathymetry using Landsat MSS data of Penang island in Malayasia. *International Journal of Remote Sensing*, 11, 557-559.

Jupp, D. L. B., 1988, Background and Extensions to Depth of Penetration (DOP) Mapping in Shallow Coastal Waters. *Symposium on Remote Sensing of the Coastal Zone*, Gold Coast, Queensland.

Kanno, A. and Tanaka, Y., 2012, Modified Lyzenga's Method for Estimating Generalized Coefficients of Satellite-Based Predictor of Shallow Water Depth. *IEEE Geoscience and Remote Sensing Letters*, 9, 715-719

Kumar, V. K., Palit, A. and Bhan, S. K., 1997, Bathymetric Mapping in Rupnarayan– Hooghly River Conuence using IRS data. *International Journal of Remote Sensing*, 18, 2269–2270.

Lillesand, T. M., Kiefer, R. W. and Chipman, J.W., 2004, Remote Sensing and Image Interpretation. New York: JohnWiley and Sons.

Lyzenga, D. R., 1978, Passive Remote Sensing Techniques for Mapping Water Depth and Bottom Features. *Applied Optics*, 17, 3, 379–383

Lyzenga, D. R., 1981, Remote Sensing of Bottom Reflectance and Water Attenuation Parameters in Shallow Water using Aircraft and Landsat data. *International Journal of Remote Sens*ing, 2, 72–82

Lyzenga, D. R., Malinas, N. R. and Tanis, F. J., 2006, Multispectral Bathymetry using a Simple Physically Based Algorithm. *IEEE Trans. Geosci. Remote Sensing*, 44, 8, 2251–2259.

Manessa, M. D. M., Kanno, A., Sekine, M., Ampou, E. E., Widagti, N., As-syakur, A. R., 2014, Shallow-Water Benthic Identification using Multispectral Satellite Imagery: Investigation on the Effects of Improving Noise Correction Method and Spectral Cover. *Remote Sensing*, 6, 4454-4472.

Muslim, A. M. and Foody, G. M., 2008, DEM and Bathymetry Estimation for Mapping a Tide-Coordinated Shoreline from Fine Spatial Resolution Satellite Sensor Imagery. *International Journal of Remote Sensing*, 29, 4515–36.

Pacheco, A., Horta, J., Loureiro, C. and Ferreira, O., 2015, Retrieval of Nearshore Bathymetry from Landsat 8 Images: A Tool for Coastal Monitoring in Shallow Waters. *Remote Sensing of Environment.* 159, 102-116.

Philpot, W. D., 1989, Bathymetric Mapping with Passive Multispectral Imagery. *Applied Optics,* 28(8), 1569-1579.

Rogers, A.S. and Kearney, M. S., 2004, Reducing Signature Variability in unmixing Coastal Marsh Thematic Mapper Scenes using Spectral Indices. *International Journal of Remote Sensing.* 25, 12, 2317–2335.

Stoffle, R. W. and Halmo, D. B., 1991, Satellite Monitoring of Coastal Marine Ecosystems: A Case from the Dominican Republic. Consortium for Integrated Earth Science Information Network (CIESIN). Saginaw, Michigan.

Stumpf, R. P., Holderied, K. and Sinclair, M., 2003, Determination of Water Depth with High-Resolution Satellite Imagery Over Variable Bottom Types. *Limnol. Oceanogr.,* 48, 2, 547–556.

Tripathi, N. K. and Rao, A. M., 2002, Bathymetric Mapping in Kakinada Bay, India, using IRS- 1D LISS-III Data. *International Journal of Remote Sensing*, 23, 6, 1013 –1025.

Van Hengel, W. and Spitzer, D., 1991, Multi-Temporal Water Depth Mapping by Means of Landsat TM. *International Journal of Remote Sensing,* 12. 4, 703-712.

Yi, G., and Li, T., 1988, The ocean information contents of remotely sensed image and the acquisition of water depth message. *Proceedings of the Ninth Asian Conference on Remote Sensing*, Bangkok, Thailand (Asian Association of Remote Sensing, University of Tokyo, Japan), F-3-1–F-3-8.

Warne, D.K., 1972, Landsat as an aid in the preparation of hydrographic charts. *Photogrammetric Engineering and Remote Sensing*, 44, 1011–16.